

Characterization of a photon pair source based on a cold atomic ensemble using a cascade level scheme

Alessandro Cerè,* Bharath Srivathsan,* Gurpreet Kaur Gulati,* Brenda Chng,* and Christian Kurtsiefer†
(Dated: December 14, 2017)

We characterize a source of photon pairs based on a cascade decay in a cold ^{87}Rb ensemble. This source is particularly suited for the generation of ~~photos~~ photons for interaction with ^{87}Rb based atomic systems. We experimentally investigate the dependence of pair generation rate, single photon heralding efficiency, and bandwidth as a function of the number of atoms, detuning and intensity of the pump beams. ~~The While the~~ power and detuning behaviors are explained by ~~an established model R. M. Whitley and J. C R Stroud, Phys. Rev. A 14, 1498 (1976), (does PRA use explicit references in abstracts? Maybe we can qualitatively describe the spirit of this work, like: early model for superradiance or something like that)~~ the steady state solution of the master equation, while the effect of the number of atoms is not fully understood yet. Measurements presented here may help optimizing this kind of photon pair sources.

I. INTRODUCTION

Time-correlated and entangled photon pairs are ~~in an~~ important resource for a wide range of quantum optics experiments, ranging from fundamental tests [1, 2] to applications in quantum information [3–5]. A common method to obtain photon pairs is Spontaneous Parametric Down Conversion (SPDC) ~~in~~ nonlinear optical crystals [6], which have proven to be extremely useful. However, photons prepared by SPDC typically have spectral bandwidths ranging from 0.1 THz to 2 THz [7, 8], making interaction with atomic systems with a lifetime-limited bandwidth on the order of few MHz difficult. Possible solutions to match the bandwidth requirements include the use of optical cavities around the crystal [9–11] and as filters [12, 13], and recently the use of miniature ~~monolithic~~ monolithic resonators made of nonlinear optical materials ~~(cite some recent Leuchs/Marquardt work)~~ [14]. A different approach uses directly atomic systems as nonlinear optical medium in the parametric process. There, a chain of near-resonant optical transitions provides an optical nonlinearity that has long been used for frequency mixing in otherwise ~~unaccessible spectral~~ unaccessible spectral domains. When two of the participating modes are not driven, such systems can be used for photon pair generation via a parametric conversion process [15, 16] ~~—(some Harris work, other more recent work?)~~ [15–17]. As the effective nonlinearity decays quickly with the distance from an atomic transition, the resulting photon pairs can be spectrally very narrow.

In this work, we investigate such a photon pair source based on four-wave mixing in a cold atomic ensemble. The resulting photon pairs are therefore directly compatible with ground state transitions of ^{87}Rb , and the pair preparation process does not suffer any reduction in

brightness caused by additional filtering. This can be interesting for preparing photon states that are fragile with respect to linear losses. A basic description of the source is presented in [18].

After the initial design and test, this source has already been used, with minor modifications, to obtain heralded single photons with exponentially rising time envelope [19, 20]. We have also studied the amount of polarization entanglement in the generated photon pairs, and observed quantum beats between possible decay paths [21]. The same source has also been used in conjunction with a separate atomic system, a single ^{87}Rb atom trapped in a far off resonant focused beam to study their compatibility [22] and the dynamics of the absorption of a single photons by an atom [23]. In those works we explored a limited range of parameters, optimized to observe the physical properties of the biphoton state of interest. In this article we present a systematic characterization of the source as function of the accessible experimental parameters. We believe that our scheme is a useful tool for the studies of the interaction of single photons and single or ensemble of atoms. In order to characterize the source, we focus our attention on generation rate, heralding efficiency, and the compromise between rates and bandwidth.

We start ~~by reviewing briefly with a brief review~~ the physical mechanism used for the generation of photon pairs, ~~then introduce the theory developed by Whitley and Stroud [24] (to explain superradiance?), followed by~~ and follow with the presentation of the experimental setup, highlighting some of its relevant and differentiating features, and a description of the measurement technique. ~~(Maybe we should give credit to the more recent work of Jen we cited earlier, just to highlight that the Stroud work was somewhat forgotten....)~~

II. FOUR WAVE MIXING IN COLD ^{87}Rb USING CASCADE DECAY

The source exploits the $\chi^{(3)}$ non-linear susceptibility of ^{87}Rb . A similar scheme was initially demonstrated

*Center for Quantum Technologies, 3 Science Drive 2, Singapore 117543

†Center for Quantum Technologies and Department of Physics, National University of Singapore, 3 Science Drive 2, Singapore 117543

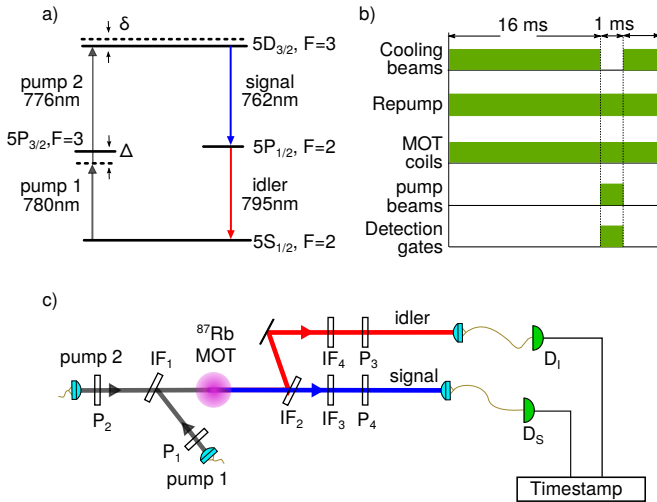


FIG. 1: (a) Cascade level scheme used for parametric conversion in atoms. (b) Timing sequence of the experiment. (c) Schematic of the experimental set up, with P1, P2, P3, and P4: Polarization filters, IF₁, IF₂, IF₃, and IF₄: interference filters, D_I, D_S: avalanche photodetectors.

with a different choice of transitions and, consequently, wavelengths [25]. The relevant electronic structure is shown in Figure 1(a). Two pump beams of wavelength 780 nm (pump 1) and 776 nm (pump 2) excite the atoms from $5S_{1/2}, F=2$ to $5D_{3/2}, F=3$ via a two-photon transition. The 780 nm pump is usually red detuned by 30 to 60 MHz Δ from the intermediate level $5P_{3/2}, F=3$ to reduce the rate of incoherent scattering, with Δ usually between 30 to 60 MHz. The two-photon detuning δ is one of the parameters we study in this work.

The subsequent decay from the excited level $5D_{3/2}, F=3$ to the ground state $5S_{1/2}, F=2$ via $5P_{1/2}, F=2$ generates pairs of photons with wavelengths centered around 795 nm (signal) and 762 nm (idler). We reject light originating from other scattering processes using narrowband interference filters. The geometry of the pump and collection modes is chosen to satisfy the phase matching condition. Energy conservation ensures time correlation of the generated photons, while the time ordering imposed by the cascade decay results in a strongly asymmetrical time envelope of the biphoton.

We already presented a model and experimental evidence of the effects of polarization choice for pumps and collection modes in a previous work [21]. In the rest of this article, the polarization of the pump beams and collection modes is chosen to maximize the effective nonlinearity and, consequently, maximize the generation rates.

III. THEORETICAL MODEL

The coherent process introduced in the previous

section This coherent process is accompanied by incoherent scattering. Both processes result in generate light at the same wavelengths making it impossible to distinguish them by spectral filtering. In As in the case of two levels systems [26, 27], coherent and incoherent scattering have different dependences for different experimental parameters [26, 27]. This is also the case for our four-level system. For a theoretical description of the two processes we follow the work of Whitley and Stroud [24]. We will see that the model describes.

To understand the difference in behavior we consider a strongly driven three-level atom [24, 28]. This simple model correctly describes some of the features of our photon pair source. With the atomic state is described by the 3×3 density matrix ρ , the dependence of the observed rates with the various parameters. We assume that the incoherent scattering rate is proportional to the most-excited state population,

$$r_{\text{inc}} \propto \langle \chi \rho_{33} \rangle, \quad (1)$$

while the signal we are interested in is proportional to the coherence generated between the most excited state and the ground state:

$$r_{\text{coh}} \propto |\langle \chi \rho_{31} \rangle|^2. \quad (2)$$

Following the procedure indicated in the appendix of [24], we derive analytical forms for an analytical solution of the steady state master equation as function of the pumps intensities (through the corresponding Rabi frequencies Ω_1 and Ω_2) and detunings (Δ and δ) [37]. In order to compare Eqs. (1) and (2) as functions of pump beams intensity and their detunings [38]. Where are these analytical forms? Can't find them. to the experimental results, we need to take into account the linewidths of the pump lasers. While each laser has a spectrum with Lorentzian profile of width ≈ 1 MHz, we assume that the combined effect of the two pumps results in a noise spectrum with Gaussian profile $G(\delta)$ of width ≈ 2 MHz. We obtain fitting functions for our results by convolving the result of the model with the combined linewidth of the pump lasers. The resulting fitting function for the single counts rates is

$$r_{\text{single}} \propto r_{\text{inc}}(\Omega_1, \Omega_2, \Delta, \delta) * G(\delta). \quad (3)$$

Similarly, the coincidences rate:

$$r_{\text{pairs}} \propto r_{\text{coh}}(\Omega_1, \Omega_2, \Delta, \delta) * G(\delta). \quad (4)$$

We define heralded efficiency the ratio:

$$\eta = \frac{r_{\text{pairs}}}{r_{\text{single}}} = \frac{r_{\text{coh}}(\Omega_1, \Omega_2, \Delta, \delta) * G(\delta)}{r_{\text{inc}}(\Omega_1, \Omega_2, \Delta, \delta) * G(\delta)}. \quad (5)$$

This model does not take into account the Zeeman manifold of the energy levels, nor the collective

interaction within the atomic ensemble. We already presented a model and experimental evidence of the effects of polarization choice for pumps and collection modes in a previous work [21]. In the rest of this article, the polarization of the pump beams and collection modes is chosen to maximize the effective nonlinearity and, consequently, maximize the generation rates. To understand the effect of collective interaction in cascaded decays process we compare our results with the model proposed in [29].

III. EXPERIMENTAL SETUP

The experimental setup is shown in Figure 1(c). The non-linear medium is an ensemble of ^{87}Rb atoms in a vacuum chamber (pressure 1×10^{-9} mbar), trapped and cooled with a Magneto-Optical trap (MOT) formed by laser beams red detuned by 24 MHz from the cycling transition $5S_{1/2}, F=2 \rightarrow 5P_{3/2}, F=3$, with a diameter of 15 mm and an optical power of 45 mW per beam. An additional laser tuned to the $5S_{1/2}, F=1 \rightarrow 5P_{3/2}, F=2$ transition optically pumps the atoms back into the $5S_{1/2}, F=2$ level. The low temperature of the ensemble ensures a negligible Doppler broadening of the atomic transition line, resulting in a reduction of the bandwidth of the generated photons by an order of magnitude compared to the hot vapor sources [30, 31].

In its initial implementation [18], the source was non-collinear, i.e., the pumping and collection modes do not lie on the same axis. This approach was chosen to minimize the collection of any pump light into the parametric fluorescence modes. In subsequent experiments we chose instead a collinear configuration. This geometry simplifies the alignment and allows for a more efficient coupling of the generated photons into single mode fibers. We combine the pump beams (780 nm and 776 nm) using a narrowband interference filter (IF₁) as a dichroic mirror. Similarly, we separate signal (762 nm) and idler (795 nm) modes using another interference filter (IF₂). Leaking of pump light into the collection modes is reduced by adding an additional interference filter in each collection mode (IF₃, IF₄). All the interference filter used in the setup have a full width half maximum bandwidth of 3 nm and a peak transmission 96% at 780 nm. We tune the transmission frequency by adjusting the angle of incidence. Polarizers P₁ and P₂ fix the polarization for the fluorescence before collecting it into single mode fibers with aspheric lenses. Single photons are detected using avalanche photo diodes (APD) with quantum efficiency of $\approx 50\%$.

Figure 1(b) shows the timing sequence used in the experiment: 16 ms of cooling of the atomic vapors, followed by a 1 ms time window, during which the cooling beams are off and pump 1 and pump 2 shine on the cloud. We use external-cavity laser diodes (ECDL) with bandwidths in the order of 1 MHz to generate the pumps, and control their power and detuning using acusto-optic modulators

(AOM).

IV. DETECTION OF PHOTON PAIRS

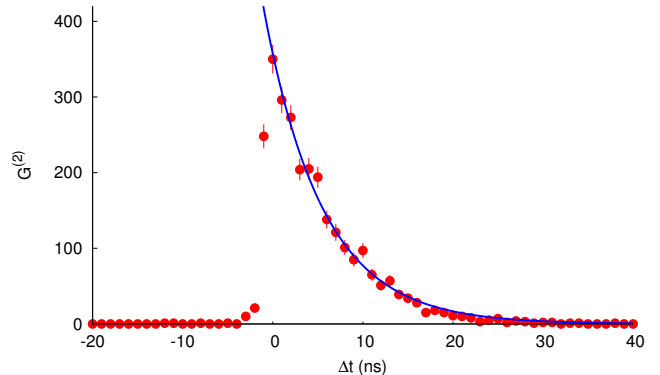


FIG. 2: Histogram of coincidence events $G^{(2)}(\Delta t)$ as a function time difference between the detection of signal and idler photons for an Total integration time 42 s. Pump powers: $P_{780} = 450 \mu\text{W}$ and $P_{776} = 3 \text{ mW}$. Two-photon detuning $\delta = 12 \text{ MHz}$. The solid line is a fit to the model described by Eq. 6, giving a value of $\tau_0 = 6.52 \pm 0.04 \text{ ns}$.

We characterize the properties of the source from the statistics and correlation of detection times for events in the signal and idler modes. All detection events are timestamped with a resolution of 125 ps. Figure 2 shows a typical coincidence histogram $G^{(2)}$, i.e., the coincidence counts as a function of the delay between detection times Δt . The correlation function shows an asymmetric shape: a fast rise followed by a long exponential decay. The rise time is limited by the jitter time of the APDs (typical value $\approx 800 \text{ ps}$), while the decay is function of the coherence time. In a previous work [18] we showed that the bandwidth is inversely proportional to the decay time constant τ . We measure τ by fitting the histogram $G^{(2)}$ with the function:

$$G_{\text{fit}}^{(2)}(\Delta t) = G_{\text{acc}} + G_0 e^{-\Delta t/\tau} \Theta(\Delta t) \quad (6)$$

where G_{acc} is the rate of accidental coincidences, Θ is the Heaviside step function, G_0 an amplitude. The rate of accidentals G_{acc} is fixed by considering the average of $G^{(2)}$ for times much larger than the coherence time, leaving as free parameters only G_0 and τ .

To characterize the source, we consider the rate of single event detection in the signal (r_s) and idler (r_i) modes, together with the rate of coincidence detection (r_p), the signature of photon pairs. In order to take into account the duty cycle of the system, all reported rates are instantaneous.

The total pair detection rate r_p of the source is obtained integrating $G^{(2)}(\Delta t)$ over a coincidence time window $0 < \Delta t < \Delta t_c$. We choose $\Delta t_c = 30 \text{ ns}$, to ensure

the collection of a large fraction of events also for the largest coherence times τ observed.

Another parameter we extract from the measured $G^{(2)}(\Delta t)$, is heralding efficiency. Due to the intrinsic asymmetry of the process, from the same measurement we define a two heralding efficiency, one for the signal:

$$\eta_S = r_p / (r_S - d_S), \quad (7)$$

and one for the idler:

$$\eta_I = r_p / (r_I - d_I). \quad (8)$$

where $d_S = 520 \text{ s}^{-1}$ and $d_I = 200 \text{ s}^{-1}$ are the dark counts rates on the signal and idler detectors.

V. EFFECT OF THE NUMBER OF ATOMS

One of the parameters of interest is the number of atoms N participating in the four-wave mixing process. We control it by varying the optical power of the repump light during the cooling phase, thus changing the atomic density without altering the geometry.

We estimate N by measuring the optical density (OD) of the atomic ensemble for light resonant with the $5S_{1/2}, F=2 \rightarrow 5P_{3/2}, F=3$ transition. To obtain a reliable measure of the OD, we turn off pump 2 and set pump 1 to $10 \mu\text{W}$, more than 40 times lower than the saturation intensity of the transition of interest. We record the transmission of pump 1 through the vacuum cell for a range of values of Δ wide enough to capture the entire absorption feature, and normalized it to the transmission observed without atomic cloud. We fit the result of the scan with the expected transmission spectrum

$$T(\Delta) = \exp\left(-\text{OD} \frac{\gamma^2}{\Delta^2 + \gamma^2}\right), \quad (9)$$

where $\gamma = 6.067 \text{ MHz}$ and OD is the only free parameter. From the size of the probe beam $w_0 \approx 450 \mu\text{m}$, we estimate N . We observed a minimum of $N \approx 1.5 \times 10^7$, corresponding to an $\text{OD} \approx 7$, to a maximum of $N \approx 6.3 \times 10^7$, $\text{OD} \approx 29$. We expect the effective number of atoms participating in the FWM process to decrease during the measurement due to the heating caused by the intense pumps.

In figure 5, we observe the shortening of decay time τ as OD increases. The measured coherence time is always shorter than $\tau_0 = 27 \text{ ns}$, expected for the spontaneous decay in free space of this transition for ^{87}Rb . This is a signature of collective effects in the cold atomic cloud [18, 32]. The solid blue line is a fit to the theoretical model proposed in [29]:

$$\tau = \frac{\tau_0}{1 + \mu \text{OD}}, \quad (10)$$

where the free parameter μ is a geometrical constant depending on the shape of the atomic ensemble.

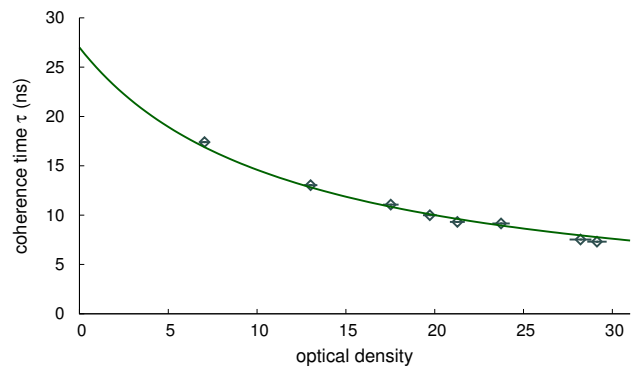


FIG. 3: Decay time of the photon pair as a function of the optical density (OD) of the atomic cloud. The solid line is obtained by fitting Eq. (10), obtaining $\mu = 0.0827 \pm 0.002$. Other parameters: $P_{776} = 15 \text{ mW}$, $P_{780} = 300 \mu\text{W}$, $\Delta = -60 \text{ MHz}$, $\delta = 12 \text{ MHz}$.

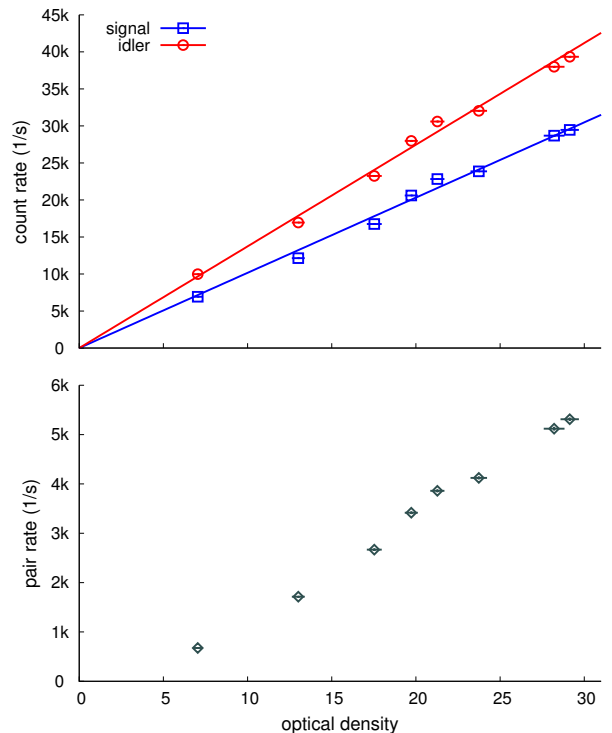


FIG. 4: Rate of single counts in the signal and idler modes (top), and rate of coincidence counts (bottom) as a function of the optical density (OD) of the atomic cloud. The solid lines are fits for $r_{s,i} = a_{s,i} \text{OD}$, with $a_{s,i}$ the only free parameter. Other parameters: $P_{776} = 15 \text{ mW}$, $P_{780} = 300 \mu\text{W}$, $\Delta = -60 \text{ MHz}$, $\delta = 12 \text{ MHz}$.

Single detection rates for the signal (r_s) and idler (r_i) modes, Fig. 4, increase linearly with the number of atoms involved in the process, as expected for incoherent processes. Instead the increase of pair rate r_p with N is faster than linear.

We do not have a complete explanation for this behavior, but we gain some insight into it by looking at

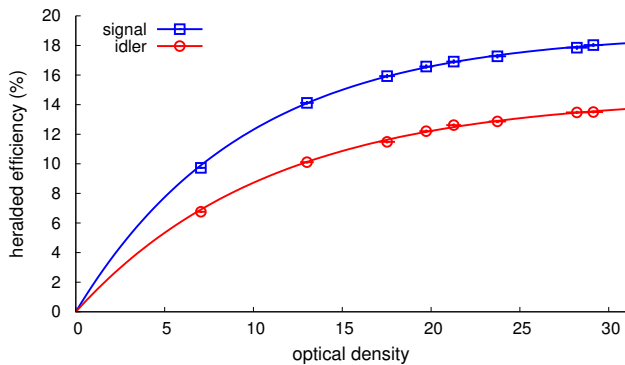


FIG. 5: Heralding efficiency for signal and idler modes as a function of the optical density. The solid lines are fits of Eq. (11) with $\eta_{0s} = 0.190 \pm 0.001$ and $OD_{0s} = 9.7 \pm 0.1$, and $\eta_{0i} = 0.150 \pm 0.001$ and $OD_{0i} = 11.3 \pm 0.2$. Other parameters: $P_{776} = 15$ mW, $P_{780} = 300 \mu\text{W}$, $\Delta = -60$ MHz, $\delta = 12$ MHz.

the heralding efficiencies, Fig. 5. Both heralding efficiencies η_s and η_i exhibit a saturation behavior that is well described by:

$$\eta_j = \eta_{0j} \left[1 - \exp\left(-\frac{OD}{OD_{0j}}\right) \right] \quad \text{with } j = s, i, \quad (11)$$

where η_{0j} and OD_{0j} are free parameters. This heuristic fit suggests that increasing the optical density of the atomic cloud allows an increase in pair rate, at the expenses of a broader photon bandwidth, but for large enough OD there is no improvement of heralding efficiency.

VI. RATES AND HERALDED EFFICIENCIES

Brightness, a usual parameter to characterize a photon pair source, is defined as the experimentally accessible rate per mW of pump power of photon pairs emitted into the desired modes. In the case of our source saturation effects of the atomic transitions involved give rise to a non-linear correlation between pumps power and rates. We report directly the instantaneous singles, r_s and r_i , and pair rates r_p as function of pump powers in Fig. 6 and 7.

For a fixed detuning δ , all rates show a saturation behavior, ~~confirmed also by the theory (solid lines in Fig. 6 and 7).~~ This suggests that it is not sufficient to increase the pump power to increase the observed pair rate. An alternative solution is to increase the number of atoms of the ensemble, but, as observed in the previous section, this comes at the expense of a larger bandwidth. As the power increases, the model predicts the saturation, but fails to reproduce the experimental results. This is probably due to the optical pumping caused by the intense pump beams.

In Fig. 8 we present the detected and predicted heralded efficiencies. For low pump powers we expect higher

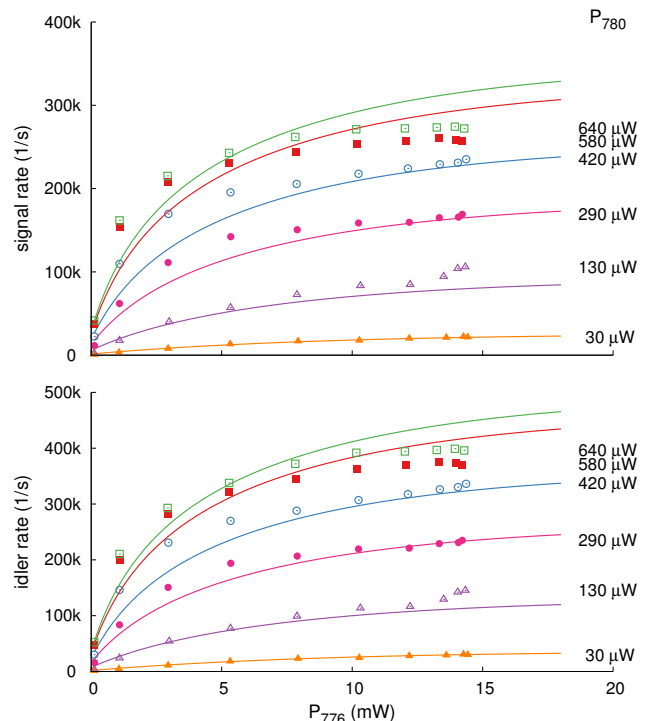


FIG. 6: Single rates for the signal (top) and idler (bottom) as function of pump power at 776 nm (P_{776}) for different pump powers at 780 nm. The vertical error bar on each point is smaller than the size of the data points. ~~The solid lines are calculated from the theory.~~ Other parameters: $OD = 29$, $\Delta = -60$ MHz, $\delta = 3$ MHz. The solid lines are numerical fits of Eq.3.

efficiency. ~~The, and the~~ experimental result confirm the trend, but do not match the theory. The calculated expected values do not take into account the full geometry of the process, i.e. atomic density profile of the cloud, intensity profile of the pump beams. We suspect this is the main source of mismatch in the high efficiency region.

A possible strategy to optimize the source brightness and heralding efficiency emerges from Fig. 7 and 8: a weak P_{780} to ensure high efficiency, and an intense P_{776} to increase brightness. The obvious limitation to this strategy is the available P_{776} : after an initial steep rise ($P_{776} < 5$ mW), the total pair generation increase slowly with increase of P_{776} .

Singles and pair rates have a strong dependence on two-photons detuning δ . Figure 9 shows that both singles and pair rates peak at $\delta \approx 0$, as expected for a scattering process. The two-steps nature of the process leads to asymmetries in the peaks, as predicted by the theory. In order to take into account the linewidth of the pump lasers (≈ 1 MHz each) we convolve the theoretical result with a Gaussian function.

Heralded efficiencies, Fig. 10, show an asymmetric dip for $\delta \approx 0$. This dip can be understood taking into account that the observed single rate is the combination of FWM,

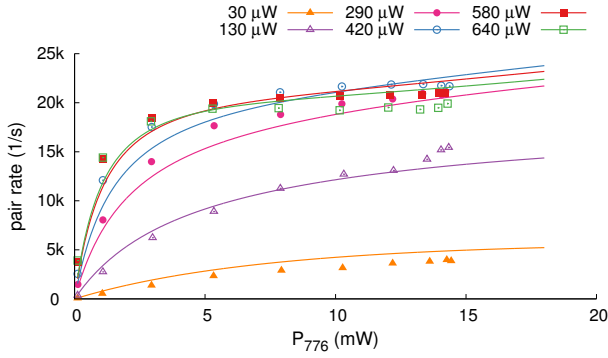


FIG. 7: Pair rates as function of pump power at 776 nm (P_{776}) for different pump powers at 780 nm. The vertical error bar on each point is smaller than the size of the data points. The solid lines are calculated from the theory. Other parameters: $OD = 29$, $\Delta = -60$ MHz, $\delta = 3$ MHz. The solid lines are numerical fits of Eq.4.

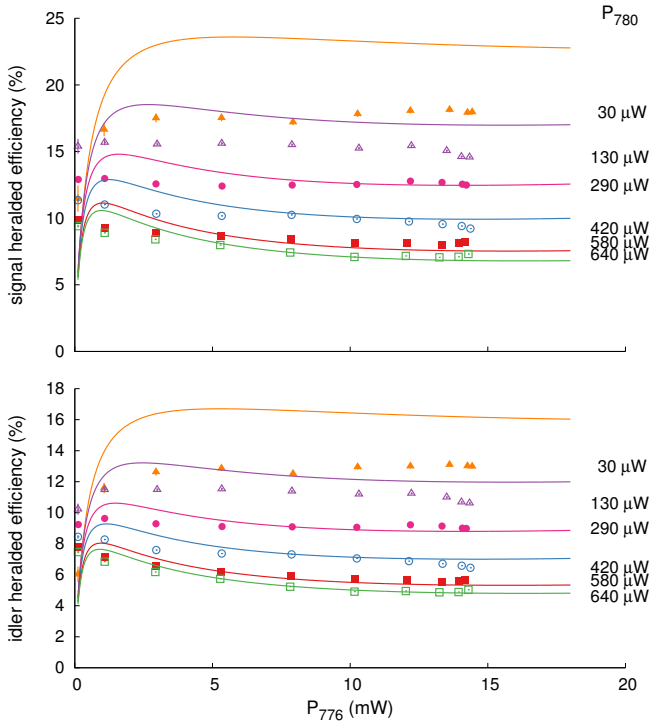


FIG. 8: Heralded efficiency as function of P_{776} for the signal (top) and idler (bottom) for different P_{780} . The vertical error bar on each point is smaller than the size of the data points. Other parameters: $OD=29$, $\Delta = -60$ MHz, $\delta = 3$ MHz. The solid lines are a numerical fit of Eq.5.

a coherent process, and incoherent scattering, with the later growing faster as δ approaches 0. When choosing the operation parameter, it is then necessary to consider what is the optimal compromise between pair rate and efficiency.

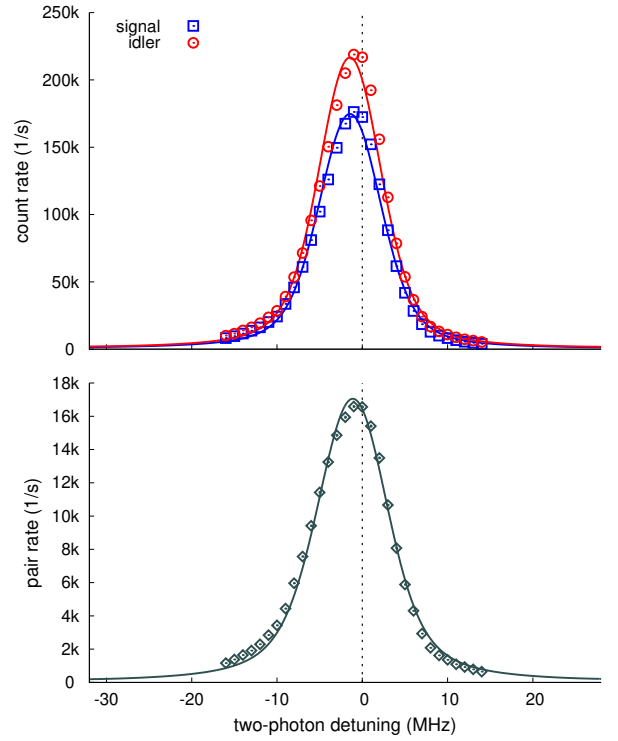


FIG. 9: (Top) Single count rates as a function of the detuning from the two photon resonance δ . The solid lines are numerical fits of Eq.3. (Bottom) Pair rate (r_p) as a function of δ . The solid line is a numerical fit of Eq.4. Other parameters: $P_{776} = 15$ mW, $P_{780} = 450$ μ W, $\Delta = -60$ MHz, $OD=29$. The dotted line indicates $\delta = 0$.

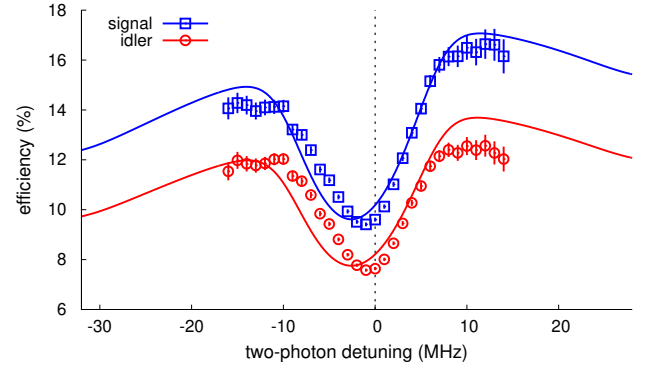


FIG. 10: Efficiency of the source as a function of the detuning from the two photon resonance δ . Other parameters: $P_{776} = 15$ mW, $P_{780} = 450$ μ W, $\Delta = -60$ MHz, $OD=29$. The solid lines are numerical fits of Eq.5. The dotted line indicates $\delta = 0$.

VII. COINCIDENCE TO ACCIDENTAL RATIO (CAR)

A relevant parameter for characterizing the usefulness of a source of photon pairs is the coincidence to accidental

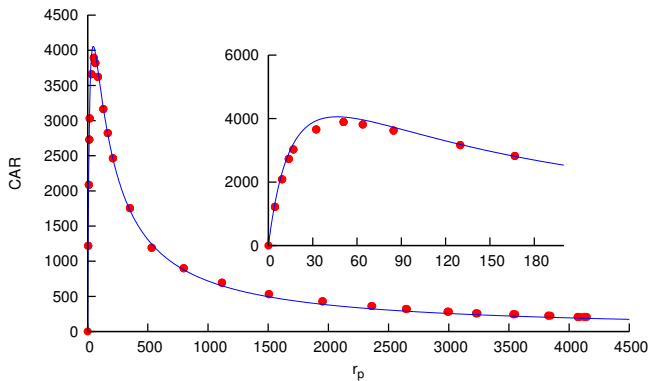


FIG. 11: The coincidence to accidental ratio (CAR) as a function of pair rates r_p . The solid line is obtained from Eq. (13) with $\eta_S = 17\%$, $\eta_I = 13\%$, $d_S = 200 \text{ s}^{-1}$, $d_I = 520 \text{ s}^{-1}$, $\Delta t = 30 \text{ ns}$, $\delta = 12 \text{ MHz}$. The inset shows a zoom of the same plot. The vertical error bar on each point is smaller than the size of the data points.

ratio (CAR) [33, 34]

$$\text{CAR} = \frac{R_p}{r_a} = \frac{r_I r_S \Delta t + r_p}{r_I r_S \Delta t}, \quad (12)$$

where accidental rate (r_a) is the rate of

noise photon generation that can degrade the correlation characteristics of the photon pair source.

The measured coincidence to accidental ratio (CAR) as a function of r_p is shown in Fig 11. We vary the pair r_p by varying P_{776} . We observe an increase in CAR when P_{776} is reduced. This is because both r_p and r_a decreases with P_{776} but drop in r_a is much faster. We observe a CAR peak at 3800 with a r_p of 50 s^{-1} . With a further decrease in r_p , CAR starts to decrease as the noise (r_a) becomes dominant. When the pump beams are blocked, r_p vanish completely. At this point we are limited only by the background noise and detector's dark counts that contribute to the singles to the detectors in signal and idler mode.

As illustrated in Fig. 8, the signal and idler heralding efficiency of the source remains almost constant as a function of P_{776} . Therefore, to fit the experimental data, we modify Eq. 12, replacing the singles rate with heralding efficiencies to

$$\text{CAR} = \frac{\left(\frac{r_p}{\eta_S} + d_S\right) \left(\frac{r_p}{\eta_I} + d_I\right) \Delta t + r_p}{\left(\frac{r_p}{\eta_S} + d_S\right) \left(\frac{r_p}{\eta_I} + d_I\right) \Delta t}. \quad (13)$$

VIII. COHERENCE TIME OF THE GENERATED PAIRS

From the theoretical models of [29], we only expect changes in the coherence times of the generated photon pairs when we change the number of atoms involved in

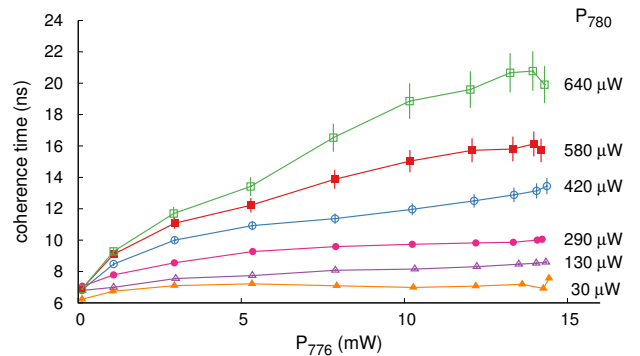


FIG. 12: Coherence time as function of pump powers. Other parameters: $\text{OD} = 29$, $\Delta = -60 \text{ MHz}$, $\delta = 3 \text{ MHz}$.

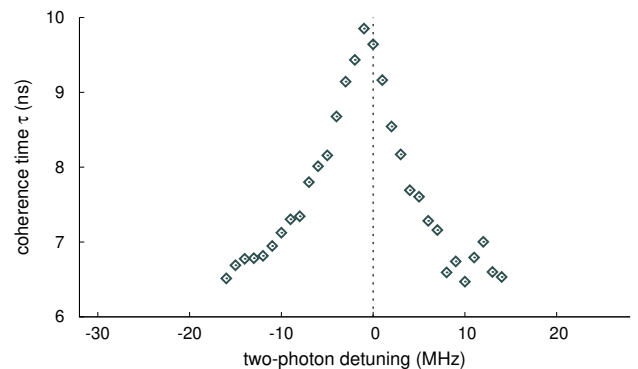


FIG. 13: Coherence time as function of detuning. Other parameters: $P_{776} = 15 \text{ mW}$, $P_{780} = 450 \mu\text{W}$, $\Delta = -60 \text{ MHz}$, $\text{OD} = 29$. The dotted line indicates $\delta = 0$.

the four-wave mixing process. In our experimental realization, we observed notable changes in τ as function of pump powers P_1 , P_2 , and detuning δ , as shown in Fig. 12 and Fig. 13.

This is mostly due to alternative decay paths to the one we considered so far. Some of these decay paths result in population transfer from $5S_{1/2}, F=2$ to $5S_{1/2}, F=1$, effectively depleting the number of atoms interacting with the pump beams. This depletion increases with pump intensities, and decreases with detuning, and is not completely neutralized by the repump beam. As a result, the observed coherence time is a mixture of decay times corresponding to different optical densities as the populations is transferred during the measurement time window.

It should be possible to optimize the efficiency of the repump during the measurement windows, thus maintaining the atomic population constant during long measurement windows. As an alternative, it is possible to optimize the duty cycle by increasing the frequency and reducing the duration of the measurement interval.

IX. CONCLUSION

In this work we presented an experimental study of the effect of two-photons detuning, pump intensity, and number of atoms on generation rates and bandwidth of photon pairs from four-wave mixing in a cold ensemble of rubidium atoms. The study is useful to understand how to set the different parameters to better exploit the source characteristics, in particular when combined with other, generally very demanding, atomic systems [22, 23].

The effect of pumps power and detunings are compatible with the theoretical model presented by Whitley and Stroud [24]. An increase in pump power corresponds to an increase to pair and singles rates, until a saturation level, with heralded efficiency determined mostly by the ground-state resonant pump. We also study how the coincidence to accidentals rate (CAR) changes as function of the generated pair rates. All rates increase with a reduction of the two-photons detuning at the expenses of heralding efficiency. This is well captured by the model, and can be intuitively explained as the result of competition between coherent and incoherent scattering processes excited by the same optical pumps.

One of the attractive aspects of cold-atoms based source is their frequency characteristics: the generated pairs are usually resonant or close to resonant and width

bandwidth of the same order of magnitude of atomic transitions. In our source the central wavelengths are fixed, the bandwidth instead is a function of the experimental parameters, in particular of the number of atoms. The dipole-dipole interaction between atoms give rise to superradiance [35], as evidenced by the reduction of coherence time as the number of atoms increases [29]. But the total number of atoms is also a function of duration, intensity, and detuning of the pump beams because of optical pumping. The dynamics of the combined effect of collective interaction between atoms and optical pumping increases the complexity of the phenomenon, and we currently do not have a model that fully explain our result. Nonetheless the experimental measurement are a useful guide to choose the number of atoms, together with the other parameters, that optimizes the specific properties desired from the source: rate, heralding efficiency, or bandwidth.

X. ACKNOWLEDGMENTS

A.C. thanks Mathias A. Seidler, Matthias Steiner, and Chin Yue Sum for useful ~~conversation regarding the best approach for a~~ discussions about the theoretical modeling of the source.

-
- [1] J. F. Clauser and A. Shimony, Rept.Prog.Phys. **41**, 1881 (1978), URL <http://stacks.iop.org/0034-4885/41/i=12/a=002?key=crossref.bb1c701ae80c3d9fd26255c1cb60fd7c>.
- [2] A. Aspect, P. Grangier, and G. Roger, Phys. Rev. Lett. **47**, 460 (1981), URL <http://dx.doi.org/10.1103/PhysRevLett.47.460>.
- [3] A. K. Ekert, Phys. Rev. Lett. **67**, 661 (1991), URL http://prl.aps.org/abstract/PRL/v67/i6/p661_1.
- [4] D. Bouwmeester, J.-W. Pan, K. Mattle, M. Daniell, A. Zeilinger, and H. Weinfurter, Nature **390**, 575 (1997), URL <http://www.nature.com/nature/journal/v390/n6660/abs/390575a0.html>.
- [5] D. Boschi, S. Branca, F. De Martini, L. Hardy, and S. Popescu, Phys. Rev. Lett. **301**, 1121 (1998), URL http://prl.aps.org/abstract/PRL/v80/i6/p1121_1.
- [6] D. C. Burnham and D. L. Weinberg, Phys. Rev. Lett. **25**, 84 (1970), URL <https://link.aps.org/doi/10.1103/PhysRevLett.25.84>.
- [7] P. G. Kwiat, K. Mattle, H. Weinfurter, A. Zeilinger, A. V. Sergienko, and Y. Shih, Phys. Rev. Lett. **75**, 4337 (1995), URL <http://link.aps.org/doi/10.1103/PhysRevLett.75.4337>.
- [8] C. Kurtsiefer, M. Oberparleiter, and H. Weinfurter, Phys. Rev. A **64**, 023802 (2001), URL <http://link.aps.org/doi/10.1103/PhysRevA.64.023802>.
- [9] C. E. Kuklewicz, F. N. C. Wong, and J. H. Shapiro, Phys. Rev. Lett. **97**, 223601 (2006), URL <http://link.aps.org/doi/10.1103/PhysRevLett.97.223601>.
- [10] F. Wolfgramm, X. Xing, A. Cerè, A. Predojević, A. M. Steinberg, and M. W. Mitchell, Opt. Express **16**, 18145 (2008), URL <http://www.opticsinfobase.org/abstract.cfm?URI=oe-16-22-18145>.
- [11] J. Fekete, D. Rielander, M. Cristiani, and H. de Riedmatten, Phys. Rev. Lett. **110**, 220502 (2013), URL <http://link.aps.org/doi/10.1103/PhysRevLett.110.220502>.
- [12] J. S. Neergaard-Nielsen, B. M. Nielsen, B. M. Nielsen, H. Takahashi, A. I. Vistnes, and E. S. Polzik, Opt. Express **15**, 7940 (2007), URL <http://www.osapublishing.org/viewmedia.cfm?uri=oe-15-13-7940&seq=0&html=true>.
- [13] A. Haase, N. Piro, J. Eschner, and M. W. Mitchell, Opt. Lett. **34**, 55 (2009), URL <http://www.opticsinfobase.org/abstract.cfm?id=175558>.
- [14] G. Schunk, U. Vogl, F. Sedlmeir, D. V. Strelakov, A. Otterpohl, V. Averbchenko, H. G. L. Schwefel, G. Leuchs, and C. Marquardt, Journal of Modern Optics pp. 1–16 (2016), URL <http://www.tandfonline.com/doi/full/10.1080/09500340.2016.1148211>.
- [15] D. A. Braje, V. Balić, S. Goda, G.-Y. Yin, and S. E. Harris, Phys. Rev. Lett. **93**, 183601 (2004), URL <http://link.aps.org/doi/10.1103/PhysRevLett.93.183601>.
- [16] D. N. Matsukevich, M. Bhattacharya, S. Y. Lan, S. D. Jenkins, and A. Kuzmich, Phys. Rev. Lett. **95**, 040405 (2005), URL <http://link.aps.org/doi/10.1103/PhysRevLett.95.040405>.
- [17] J. F. Chen and S. Du, Front. Phys. **7**, 494 (2012), URL <http://link.springer.com/10.1007/s11467-012-0260-1>.
- [18] B. Srivathsan, G. K. Gulati, B. Chng, G. Maslennikov, D. N. Matsukevich, and C. Kurtsiefer, Phys. Rev. Lett. **111**, 123602 (2013), URL <http://journals.aps.org/>

- prl/abstract/10.1103/PhysRevLett.111.123602.
- [19] G. K. Gulati, B. Srivathsan, B. Chng, A. Cerè, D. Matsukevich, and C. Kurtsiefer, Phys. Rev. A **90**, 033819 (2014), URL <http://link.aps.org/doi/10.1103/PhysRevA.90.033819>.
- [20] B. Srivathsan, G. K. Gulati, A. Cerè, B. Chng, and C. Kurtsiefer, Phys. Rev. Lett. **113**, 163601 (2014), URL <http://journals.aps.org/libproxy1.nus.edu.sg/prl/abstract/10.1103/PhysRevLett.113.163601>.
- [21] G. K. Gulati, B. Srivathsan, B. Chng, A. Cerè, and C. Kurtsiefer, New J. Phys. **17**, 093034 (2015), URL <http://iopscience.iop.org/libproxy1.nus.edu.sg/article/10.1088/1367-2630/17/9/093034>.
- [22] V. Leong, S. Kosen, B. Srivathsan, G. K. Gulati, A. Cerè, and C. Kurtsiefer, Phys. Rev. A **91**, 063829 (2015), URL <http://link.aps.org/doi/10.1103/PhysRevA.91.063829>.
- [23] V. Leong, M. A. Seidler, M. Steiner, A. Cerè, and C. Kurtsiefer, Nat Comms **7**, 13716 (2016), URL <http://www.nature.com/libproxy1.nus.edu.sg/ncomms/2016/161129/ncomms13716/full/ncomms13716.html>.
- [24] R. M. Whitley and J. C. R. Stroud, Phys. Rev. A **14**, 1498 (1976), URL <https://link.aps.org/doi/10.1103/PhysRevA.14.1498>.
- [25] T. Chanelière, D. N. Matsukevich, and S. D. Jenkins, Phys. Rev. Lett. **96**, 093604 (2006), URL <http://link.aps.org/doi/10.1103/PhysRevLett.96.093604>.
- [26] B. R. Mollow, Phys. Rev. **188**, 1969 (1969), URL <http://link.aps.org/doi/10.1103/PhysRev.188.1969>.
- [27] C. Cohen-Tannoudji, J. Dupont-Roc, and G. Grynberg, *Optical Bloch Equations* (Wiley-VCH Verlag GmbH, 1994), pp. 353–405.
- [28] S. V. Lawande, R. R. Puri, and R. D’Souza, Phys. Rev. A **33**, 2504 (1986), URL <https://link.aps.org/doi/10.1103/PhysRevA.33.2504>.
- [29] H. H. Jen, J. Phys. B: At. Mol. Opt. Phys. **45**, 165504 (2012).
- [30] R. T. Willis, F. E. Becerra, L. A. Orozco, and S. L. Rolston, Phys. Rev. A **82**, 053842 (2010), URL <http://dx.doi.org/10.1103/PhysRevA.82.053842>.
- [31] D.-S. Ding, Z.-Y. Zhou, B.-S. Shi, X.-B. Zou, and G.-C. Guo, Opt. Express **20**, 11433 (2012), URL <http://www.opticsinfobase.org/viewmedia.cfm?uri=oe-20-10-11433&seq=0&html=true>.
- [32] M. Gross and S. Haroche, Physics Reports **93**, 301 (1982), ISSN 0370-1573, URL <http://www.sciencedirect.com/science/article/pii/0370157382901028>.
- [33] H. Takesue and K. Shimizu, Opt. Commun. **283**, 276 (2010), URL <http://linkinghub.elsevier.com/retrieve/pii/S0030401809009651>.
- [34] C. Xiong, G. D. Marshall, A. Peruzzo, M. Lobino, A. S. Clark, D. Y. Choi, S. J. Madden, C. M. Natarajan, M. G. Tanner, R. H. Hadfield, et al., Appl. Phys. Lett. **98**, 051101 (2011), URL <http://scitation.aip.org/content/aip/journal/apl/98/5/10.1063/1.3549744>.
- [35] R. H. Dicke, Phys. Rev. **93**, 99 (1954).
- [36] A. V. Akimov, E. O. Tereshchenko, S. A. Snigirev, A. Y. Samokotin, A. V. Sokolov, and V. N. Sorokin, Quantum Electron. **40**, 139 (2010), URL <http://iopscience.iop.org/article/10.1070/QE2010v040n02ABEH014206>.
- [37] [These analytical forms are long and cumbersome, we have included them in the appendix. We note that the solutions presented in \[24\] contain a mistake, as already noted by \[36\]](#)
- [38] ~~[The analytical forms presented in the original papers contain a mistake, as already noted by \[36\]](#)~~